Amphiphilic Properties of Dumbbell-Shaped Inorganic−Organic−Inorganic Molecular Hybrid Materials in Solution and at an Interface

Mauricio F. Misdrahi,[†] Minghui Wang,[†] Chullikkattil P. Pradeep,[‡] Feng-Yan Li,[‡,§] Claire Lydon,[‡] Lin Xu,[§] Leroy Cronin,*,[‡] and Tianbo Liu*,[†]

[†]Department of Chemistry, Lehigh University, Bethlehem, Pennsylvania 18015, United States
[‡]WestCHEM, School of Chemistry, The University of Glasgow, University Avenue, Glasgow G12 8QQ, Scotland, U.K.
[§]Key Laboratory of Polyoxometalate Science of the Ministry of Education, Department of Chemistry, Northeast Normal University, Changchun, Jilin, People's Republic of China

ABSTRACT:
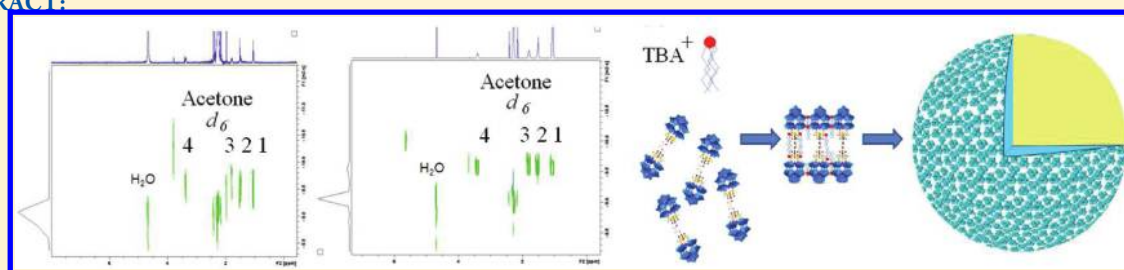
Five novel dumbbell-shaped polyoxometalate (POM)-based inorganic−organic−inorganic molecular hybrids are investigated both in polar solvents and at interfaces for potential amphiphilic properties, which are compared with those of conventional surfactants. These hybrids with the general formula $\{P_2V_3W_{15}\}_2$-bis(TRIS)-linker are formed by linking two Wells−Dawson-type clusters, $[P_2V_3W_{15}O_{62}]^{9-}$, with different linear bis(TRIS) linker ligands between the two TRIS moieties. Laser light scattering (LLS) studies reveal the presence of self-assembled vesicular structures in water/acetone mixed solvents, and the vesicle size increases with increasing acetone content, suggesting a charge-regulated process. The elastic constants, which are used to calculate the bending energy during vesicle formation, reveal that the organic ligands play an important role in determining the self-assembly process and that the hybrids do demonstrate amphiphilic behavior at the water/air interface. Furthermore, it is shown that some of the hybrids form monolayers at the interface, with an average molecular area that can be correlated with their organic linkers, as determined from their $\pi−A$ isotherms. Finally, the hybrids not only display amphiphilic behavior akin to that of a surfactant but also exhibit an unusually high entropy contribution to vesicle formation as a result of their unique large, polar head groups, complex organic linkers, and their special molecular architectures as well as because of the involvement of the amphiphilic tetrabutylammonium (TBA) counterions.

■ INTRODUCTION

Polyoxometalates (POMs) represent a large group of giant metal oxide inorganic clusters with rich physical and chemical properties and potential applications as electronic and catalytic materials.[1] The incorporation of organic components can sometimes modify the electronic properties of the POMs.[2,3] At the same time, hydrophobic organic components are added to the usually hydrophilic POM clusters and result in possible amphiphilic properties, which can increase the compatibility of the POMs in organic media. The resulting hybrid materials will combine not only the advantages of individual inorganic and organic components but also exhibit close interaction and a synergistic effect between them.[2−6] Various POM-containing hybrid materials have been synthesized in the past few years via different approaches,[7−10] some of which include diverse inorganic structures and functional organic groups.[11,12]
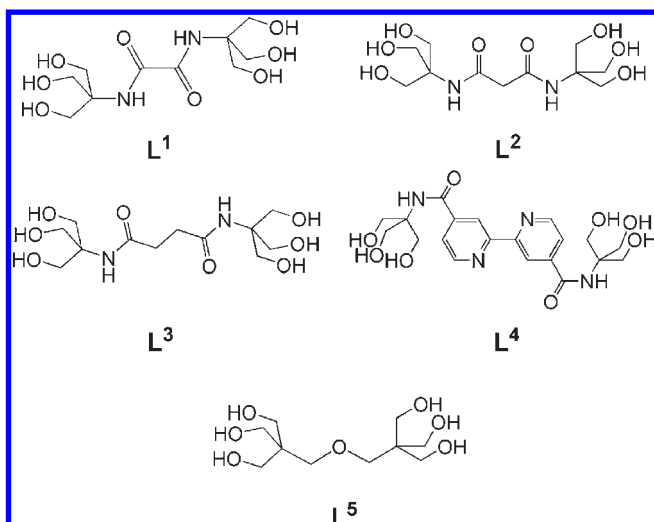
Bearing this in mind, we speculated that POM-based inorganic−organic hybrid materials might demonstrate amphiphilic features in selective solvents, and this was confirmed by some preliminary studies from different groups. In our own work, we recently showed that[13] Anderson-based hybrids $[TBA]_3$-$[MnMo_6O_{18}\{(OCH_2)_3CNHCO-(CH_2)_{n-2}CH_3\}_2]$ (where TBA = the tetrabutylammonium cation and $n = 6, 16$) slowly self-assembled into bilayer vesicular structures in mixed solvents of acetonitrile (MeCN) and water. Furthermore, the same types of hybrids can form reverse vesicles in MeCN/toluene mixed solvents.[14] Therefore, these data are direct evidence that some hybrids can be treated as novel surfactants with large, functional

Scheme 1. Diagram of Bis(TRIS) Ligands L^1–L^5 Used in This Study to Synthesize Hybrids 1–5

Table 1. Five Dumbbell-Shaped Inorganic–Organic Hybrid Molecules[a]

Molecular Formulae of Hybrids	Polar head to polar head length	Molecular Structure
TBA$_{10}$H$_2$[(P$_2$V$_3$W$_{15}$O$_{59}$(OCH$_2$)$_3$CNHCO)$_2$] (1)	4.03 nm	
TBA$_{10}$H$_2$[(P$_2$V$_3$W$_{15}$O$_{59}$(OCH$_2$)$_3$CNHCO)$_2$CH$_2$] (2)	4.12 nm	
TBA$_{10}$H$_2$[(P$_2$V$_3$W$_{15}$O$_{59}$(OCH$_2$)$_3$CNHCOCH$_2$)$_2$] (3)	4.25 nm	
TBA$_{10}$H$_2$[(P$_2$V$_3$W$_{15}$O$_{59}$(OCH$_2$)$_3$CNHCOC$_5$H$_3$N)$_2$] (4)	4.72 nm	
TBA$_{10}$H$_2$[(P$_2$V$_3$W$_{15}$O$_{59}$(OCH$_2$)$_3$CCH$_2$)$_2$O] (5)	3.35 nm	

[a] The inorganic parts are Wells–Dawson-type clusters connected by five different bis(TRIS) ligands: L^1–L^5. The second column shows approximate lengths of each hybrid. (blue ○) tungsten, (yellow ○) vanadium, (purple ○) phosphorous, (red ○) oxygen, (●) carbon, and (blue ○) nitrogen. For clarity, hydrogen is not shown.

polar head groups. Micelles and cylindrical assemblies have been observed by Landsmann et al. when they studied a hybrid surfactant with two long alkyl tails on the same side of the POM cluster.[15a] Wang et al. successfully synthesized POM–polymer hybrid materials that demonstrate amphiphilic properties by forming vesicular structures.[15b] We[16] also showed that the dumbbell-shaped hybrid TBA$_{10}$H$_2$[(P$_2$V$_3$W$_{15}$O$_{59}$(OCH$_2$)$_3$-CCH$_2$)$_2$O] (5) containing two Wells–Dawson-type clusters linked together by bis(TRIS) ligand (where TRIS = tris-(hydroxymethyl)aminomethane derivative) also formed well-defined vesicle structures in acetone/water mixed solvents. The average vesicle size can be tuned by the polarity of the solvent (i.e., dielectric constant) with larger vesicles formed in less polar solvents. Closely packed solventphobic layers are needed for bilayer vesicle formation. Considering that the dumbbells possess relatively small organic domains, we speculated that the large, amphiphilic TBA counterions played a unique role in the formation of vesicles by helping to fill the space in the hydrophobic domains of the vesicles.

Although the above preliminary studies are important, they do not yet establish a solid concept that such hybrids are indeed able to act as novel surfactants. For this to be proven, several critical issues need to be addressed in order to clarify the special features of such hybrids further and to identify their similarities to and differences from conventional surfactants: (1) consistent, predictable self-assembly behavior, which can be achieved by synthesizing and studying a series of similar hybrids and confirming that they follow similar, controllable amphiphilic behavior in solution; (2) the amphiphilic nature of such hybrids on surfaces, at interfaces, and in different solvents; and (3) a determination of the physicochemical properties of such surfactants (e.g., cmc, enthalpy, and entropy changes for the self-assembly) with a comparison to the conventional surfactants. To achieve these, we have developed a series of linear bis(TRIS) ligands containing different functional groups at the center (Scheme 1) and have used these ligands to generate a series of Wells–Dawson-type cluster-based dumbbell hybrid surfactants (1–5, formulae and structures shown in Table 1).[17] These new materials were well characterized by elemental analyses, IR and NMR spectroscopy, and ESI-MS spectrometry, and one of these dumbbell hybrids (1) was characterized by single-crystal X-ray crystallography.[16]

The X-ray crystallography and ESI-MS analyses have confirmed the formation of dumbbell-shaped hybrids 1–5. Initial studies into their thermal stability showed that these compounds were stable up to approximately 225 °C.

In this article, we report our systematic studies on the amphiphilic properties of five dumbbell-shaped Wells–Dawson hybrids 1–5 in solution and at liquid/vapor interface by exploring their self-assembly, assembly sizes, stability, thermodynamic properties, and phase behavior. We then intended to use this series of hybrids as models to demonstrate the surfactant-like properties of such hybrids and their similarities and differences with respect to the conventional surfactants due to their extraordinarily large polar head groups, limited and relatively rigid hydrophobic domains, and bulky and amphiphilic TBA counterions.

■ MATERIAL AND METHODS

Sample Preparation. The five dumbbell hybrids 1–5 were synthesized at The University of Glasgow.[16,17] Crystals or powders of each hybrid were dissolved in the proper solvent at room temperature. For acetone/water mixed solvents, the sample was first dissolved in acetone and then deionized water was added dropwise with gentle stirring until the desired solvent composition was reached. The same gentle agitation was applied overnight, and the solutions were kept at room temperature for 2 h before being studied.

Static and Dynamic Light Scattering (SLS and DLS). SLS and DLS measurements were performed by using a Brookhaven Instruments spectrometer that was equipped with two lasers operating at 532 and 633 nm, respectively. The sample solutions were filtered with 0.2 μm filter membranes into dust-free light-scattering cells. The sample chamber was thermostatted and could be controlled to within 0.1 °C. The basis of the SLS is the Rayleigh–Gans–Debye equation,[18] which is used to determine the radius of gyration (R_g) and molar mass of particles. SLS experiments were performed at scattering angles of 15–45° at 2° intervals.

For DLS measurements, the intensity–intensity time correlation function was measured by means of a BI-9000 AT multichannel digital correlator. The normalized electric field time correlation function was
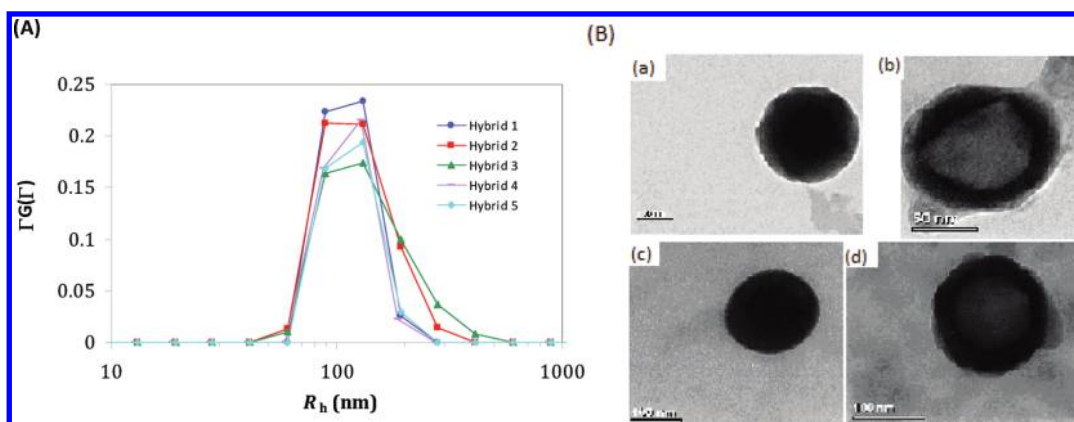
Figure 1. (A) CONTIN analysis for the DLS studies on various 1.0 mg/mL hybrid surfactants in a 50/50 vol % acetone/water mixed solvent. (B) TEM studies on the same solutions of hybrids **1**−**4** (a−d, respectively). TEM image of the vesicles formed by hybrid **5** was reported previously.[16]

then analyzed by the CONTIN method,[19] which yields information on the distribution of the characteristic line width that can be used to determine the particle's apparent diffusion coefficient D and then the average hydrodynamic radius (R_h) through the Stokes−Einstein equation

$$R_h = \frac{k_B T}{6\pi\eta_0 D} \tag{1}$$

where k_B is the Boltzmann constant, η_0 is the viscosity of the solvent, and T is the temperature of the solution. The apparent D values measured at different scattering angles are extrapolated to zero scattering angle in order to obtain $R_{h,0}$.

Transmission Electron Microscopy (TEM). The samples were prepared by pipetting 5 μL of each solution (1 mg/mL) onto a carbon-coated EM grid. The TEM studies were performed with a JEOL 2000FX microscope operating at up to 200 kV.

Zeta Potential Analysis (ζ). All ζ potential measurements were performed using a Brookhaven Instruments Zeta PALS analyzer. The sample chamber was maintained at 23 ± 0.1 °C. The instrument is equipped with a red laser operating at a 660 nm wavelength and an accuracy of ±2% for filtered samples.

Langmuir−Blodgett (L−B) Isotherms. Solutions for different hybrid surfactants were prepared in 90/10 vol % chloroform/acetonitrile at 20 °C. Deionized water (18.2 MΩ·cm, pH ∼6 after treatment with a Milli-Q water purification system) was used as the subphase. All monolayer measurements were made using a Nima 612D film balance (Nima Technologies, Coventry, England) equipped with an L−B dipper, and all isotherms were determined at 25 °C. The typical Langmuir−Blodgett procedure involved a 20 min waiting period after spreading the solutions over the water subphase before any compression was applied.

■ RESULTS AND DISCUSSION

Self-Assembly of the Wells−Dawson-Based Dumbbell Hybrids in Selective Solvents. All five dumbbell-shaped hybrids are insoluble in water but soluble in acetone and water/acetone mixed solvents, whereby the solubility varies depending on the composition of the central part of the linking groups. The solutions were monitored by an LLS technique for any possible formation of large assemblies, and all of the hybrid solutions were observed to reach equilibrium within 24 h, after which there was no further change in the solution for up to 90 days.

Formations of supramolecular structures by the five hybrids are observed in acetone/water (20−70 vol % acetone) solutions. SLS studies reveal strong scattering intensities from such
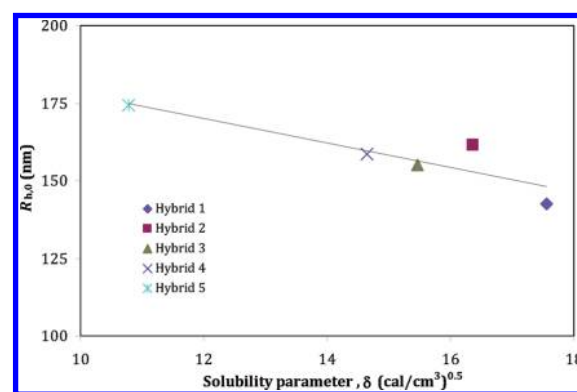

Figure 2. Relation between the vesicle size (in a 50/50 vol % water/acetone mixed solvent) and the polarity of the organic linkers as calculated by the Small method.

solutions (>2000 kcps at a 90° scattering angle; for comparison, benzene has an intensity of 110 kcps), and DLS studies reveal narrow particle size distributions of large structures with an average R_h of over 100 nm depending on the type of hybrid (Figure 1A). For each type of hybrid, the large assemblies show a simple relation of $R_g/R_{h,0} \approx 1$ (R_g was measured by an SLS technique). For spherical objects (evidence from TEM studies, Figure 1B), this indicates a hollow vesicular structure[20] similar to that in our previous study[16] on hybrid **5**. TEM studies further confirm the formation of vesicular structures in hybrid solutions (Figure 1B). Therefore, it is possible to conclude that the various dumbbell-shaped hybrid surfactants self-assemble into vesicles in water/acetone mixed solutions. It is also reasonable to hypothesize that the dumbbell hybrids use their two polar POM clusters to face the hydrophilic solvent but use their organic linkers to form the hydrophobic domain. This initial study confirms that all of the hybrids form vesicles in similar solvents.

The vesicle sizes from the five hybrids are relatively similar, but minor differences can still be identified (Figures 1 and 2) relating to the organic linker part as expected. The solubility parameter (δ) is widely used to estimate the degree of hydrophobicity of organic components[21,22] (e.g., the Small method[23] for polymers). It is based on the addition of the attraction constants for all organic groups, and the δ value is determined by the energy of vaporization and molar volume of each organic group. With this approach, the effect of the hydrophobicity of the middle organic
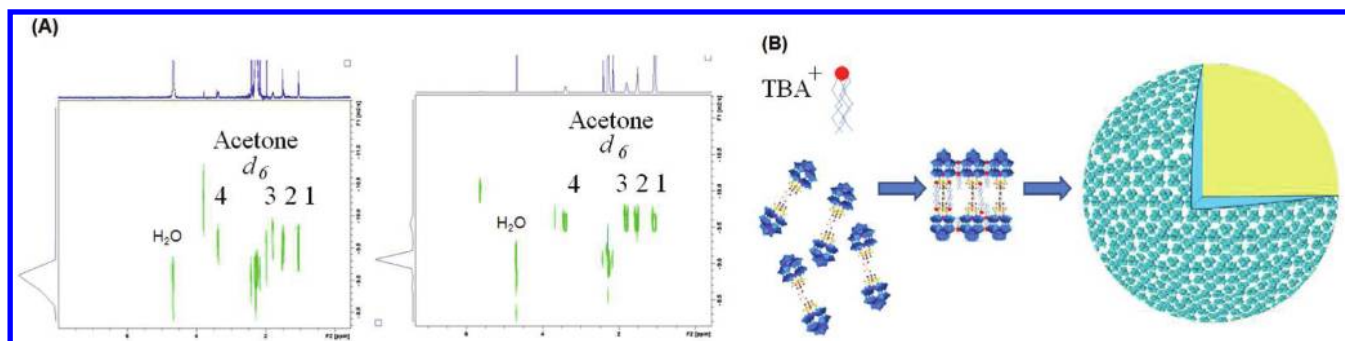
Figure 3. (A) ^{1}H DOSY was used to infer the TBA binding to the polar heads. The first experiment shows the D_2O, acetone-d_6, and TBA signals. (B) Cartoon of vesicle formation occurring in the presence of hybrid surfactants and the TBA countercation in water/acetone mixtures.
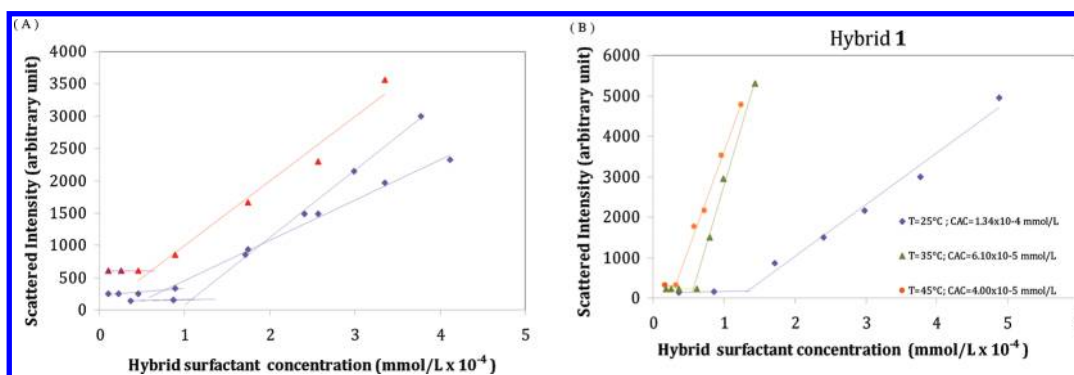

Figure 4. Determination of the cac value for (A) hybrids **1**−**3** in a 50/50 vol % water/acetone mixed solvent at 25 °C. The corresponding values are (**1**) 1.34×10^{-4} mmol/L, (**2**) 0.89×10^{-4} mmol/L, and (**3**) 0.45×10^{-4} mmol/L. Determination of the cac value for (B) hybrid **1** in a 50/50 vol % water/acetone mixed solvent at different temperatures.

linker on vesicle formation can be estimated. As shown in Figure 2, the vesicle sizes formed by different hybrids decrease (slightly but monotonically) with increasing polarity of the organic part. This is reasonable because less polar organic linkers would interact with each other more closely and induce a more compact solvent-phobic layer, leading to vesicles with smaller curvatures or larger sizes. The linear relationship in Figure 2 indicates that the five hybrids follow very similar mechanisms with respect to assembly behavior in polar solvents.

State of Counter Cations (TBA) in Vesicle Formation. A ^{1}H NMR DOSY experiment was performed to determine the diffusion coefficients of protons in solution to confirm the binding between TBA and hybrids. *n*-Tetrabutyl ammonium iodide (TBAI, 1×10^{-4} M, as a reference) and hybrid **5** in a 50/50 vol % acetone-d_6/D_2O solution were prepared in order to compare the diffusion coefficients of their protons. As shown in Figure 3A, the four groups of protons from the *n*-butyl chains of TBAI have diffusion coefficients of 4.08×10^{-10}, 4.47×10^{-10}, 4.00×10^{-10}, and 3.74×10^{-10} m^2/s, respectively. However, the same proton groups from TBA in hybrid **5** have values of 2.93×10^{-10}, 3.03×10^{-10}, 2.70×10^{-10}, and 3.00×10^{-10} m^2/s, respectively, suggesting that the TBA ions move much more slowly in the presence of the hybrid vesicles. It is clear that TBA countercations are closely associated with the large vesicles as a result of electrostatic interactions.

This experiment cannot directly confirm the involvement of the alkyl chains on TBAs in the hydrophobic region because in such a case the protons will be almost immobile and will not generate any

observable signals during the NMR DOSY studies. Considering that these hybrids are different from conventional surfactants in that they have large polar headgroups, which could make the close packing of hydrophobic domains (the alkyl chains) difficult because of their spatial obstruction, we speculated that the large TBA cations might get involved in forming the hydrophobic domains.[16] Furthermore, these cations could also further effectively screen the repulsive interactions between adjacent POM clusters on the vesicle surface, as suggested schematically in Figure 3B.

Critical Association Concentration (cac) of Vesicle Formation. The cac is defined as the solute concentration at which vesicle formation starts in solution, and the SLS technique is commonly used to determine the cac by detecting a sudden, significant increase in the scattering intensity with solute concentration.[24] Figure 4A shows the cac determination for hybrids **1**−**3** at 25 °C. These three hybrids contain similar organic linkers; therefore, they can be used for comparison. It is clear that the cac value decreases with increasing methylene groups in the organic linker (i.e., the vesicle formation becomes more favored when the organic linker becomes more hydrophobic). The cac values for hybrids **4** and **5** in the same solvent are 3.5×10^{-4} and 9.2×10^{-5} mM at 25 °C, respectively, which are smaller than those for the first three hybrids. This is consistent with the solubility parameter calculations that show that the last two hybrids contain the most-hydrophobic organic linkers.
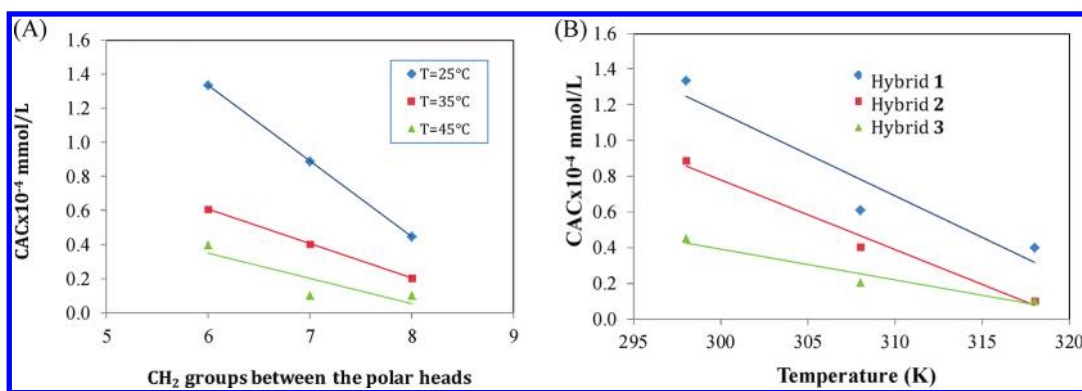
Figure 5. (A) Effect of the methylene group ($-CH_2-$) values for hybrids **1**−**3**. (B) cac values for hybrids **1**−**3** at three different temperatures in 50 vol % water/acetone.

For a given hybrid, the cac value decreases with increasing temperature, and a typical measurement is shown in Figure 4B by using **1** as an example. Figure 5B also shows the effect of temperature on the cac values for hybrids **1**−**3**, which demonstrate very similar trends. This case is similar to other entropy-driven self-assembly processes (see below), such as the micelle formation of oxyethylene alkyl chain (C_nE_m) nonionic surfactants,[25] but is opposite to enthalpy-driven processes such as the case of sodium alkyl sulfonates where the cmc increased with increasing temperature.[26]

The thermodynamic parameters of vesicle formation can be obtained from the temperature dependence of the cac values, which can provide useful information about the driving force behind the self-assembly through the determination of the standard Gibbs free energy change:

$$\Delta G^{\circ}_m = RT \ln X_{cac} \qquad (2)$$

The standard enthalpy change (ΔH°_m) can be determined by the Gibbs−Helmholtz equation.[18]

$$\Delta H_m^{\circ} = -T^2 \left(\frac{\partial(\Delta G_m^{\circ}/T)}{\partial T} \right)_P \qquad (3)$$

The entropy change (ΔS°_m) can be calculated by the Gibbs relation[24]

$$\Delta S_m^{\circ} = \frac{\Delta H_m^{\circ} - \Delta G_m^{\circ}}{T} \qquad (4)$$

Table 2 summarizes the thermodynamic parameters for all five hybrids. The negative changes in ΔG°_m indicate that vesicle formation is a spontaneous process, and the positive values of ΔH°_m imply that vesicle formation is endothermic. This is quite typical of amphiphiles in polar solvents because their self-assembly process is accompanied by breaking some ordered solvent structures around hydrophobic domains, which makes the whole self-assembly process entropy-driven. Interestingly, these $T\Delta S^{\circ}_m$ values are significantly larger than those for the vesicle formation of conventional surfactants, such as the ionic Gemini surfactants.[27] We speculate that this may be attributed to the bulky TBA countercations (each hybrid has 10 TBA counterions). The TBA ions possess long hydrophobic tails that might be involved in the vesicle-formation process by destroying the hydrogen bonds formed by the

Table 2. Thermodynamic Parameters of the Vesicle Formation of Hybrids 1−5 in a 50/50 Vol % Water/Acetone Mixed Solution

hybrid	temp, °C ± 0.2	ΔG°_m, kJ/mol	ΔH°_m, kJ/mol	$T\Delta S^{\circ}_m$, kJ/mol
1	25	−48.1	44.5	92.6
	35	−51.7	47.6	99.3
	45	−54.5	50.7	105.2
2	25	−51.6	43.0	94.6
	35	−53.5	45.9	99.4
	45	−58.1	48.9	107.1
3	25	−50.8	47.2	98.0
	35	−54.5	50.4	104.9
	45	−57.6	53.7	111.3
4	25	−45.7	57.9	103.6
	35	−48.7	61.8	110.5
	45	−52.9	65.9	118.8
5	25	−49.0	39.4	88.4
	35	−51.9	42.1	94.0
	45	−55.1	44.9	100.0

well-organized water molecules around the alkyl tails and increasing the entropy of the system. In addition, the length of the organic linker may show a direct relation to the $T\Delta S^{\circ}_m$ value, as for a longer linker the entropy gain tends to be more negative because more hydrogen bonds need to be broken (Figure 6).

Surface Charge Regulates the Self-Assembly of Hybrids. For the formation of shell-like assemblies, the size of the assemblies shows a clear trend with the solvent content (in the dielectric constant) if the self-assembly process is charge-regulated, which is confirmed in different "blackberry" structures formed by hydrophilic macroions in polar solvents.[28] The bilayer vesicle formations in different solvents for the Mn-Anderson-C_{16} hybrid and for dumbbell hybrid **5**[13,16] are also charge-regulated. To go one step further, we compare the average assembly sizes of the five dumbbell hybrids under the same experimental conditions (e.g., solvent content and temperature). A linear relationship between the vesicle size and the inverse dielectric constant ($1/\varepsilon_r$) is observed for each of the five systems (Figure 7), further confirming that the five hybrids follow very similar self-assembly mechanisms. The slopes of the linear regressions shown in Figure 7 reveal the magnitude of the attractive forces among
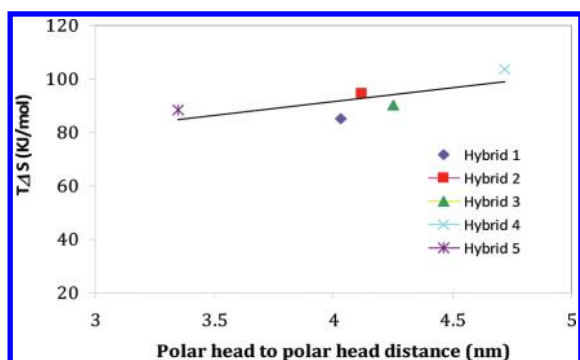
Figure 6. The entropy change for vesicle formation is related to the length of the organic linkers of the hybrids.
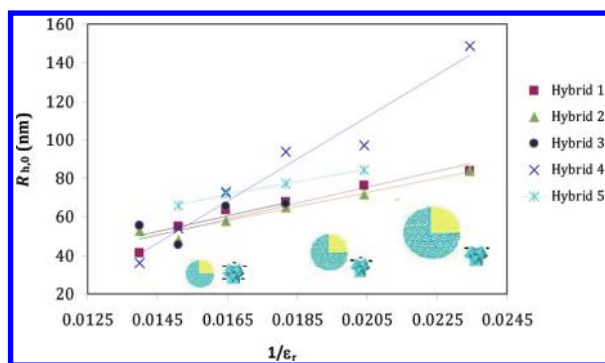

Figure 7. Linear relationship between the hybrid vesicle size and $1/\varepsilon_r$ in water/acetone mixed solvents with different compositions.

the monomers on the vesicle surface (u), first obtained in blackberries formed by {Mo_{132}} macroions[29]

$$R \approx \frac{-48\lambda_b u}{\zeta^2} \qquad (5)$$

$$\lambda_b = \frac{e^2}{4\pi\varepsilon_0\varepsilon_r k_B T} \approx \frac{56}{\varepsilon_r} \qquad (6)$$

where u, ζ, λ_b, ε_0, ε_r, e, k_B, and T are the cohesive bond energy between monomers, the zeta potential of the assemblies, the Bjerrum length, the vacuum permittivity, the relative dielectric constant of the solvent, the electron charge, the Boltzmann constant, and the absolute temperature, respectively. The u values and consequently the chemical potential ($\Delta\mu°$) for the vesicle formation of five hybrids are calculated for comparison from the slopes in Figure 7 (summarized in Table 3). $\Delta\mu°$ is calculated by assuming a hexagonal arrangement of monomers on the vesicle surface; therefore, $\Delta\mu° = 3u$.[30]

The cohesive bond energy can also be calculated from cac values. For example, for hybrid **5**, the cac is 4.71×10^{-9} mol/L at 25 °C in a 50/50 vol % acetone/water mixed solvent. By assuming that vesicles consist of the predominantly hexagonally arrayed packing of hybrid molecules, the cohesive bond energy (u) can be calculated as $-7.80k_B T$ from[30]

$$X_{cac} \approx e^{n_b u/k_b T} \qquad (7)$$

where n_b is the average number of bonds per molecule (three here). This result is very close to our previous result of $-7.50k_B T$

Table 3. Zeta Potential (ζ), Cohesive Bond Energy (u), and Chemical Potential ($\Delta\mu°$) of Vesicle Formation for All Five Dumbbell Hybrids in a 50/50 Vol % Acetone/Water Mixed Solvent

dumbbell hybrid	ζ, $k_B T$	u, $k_B T$	$\Delta\mu°$, $k_B T$
Hybrid **1**	−0.7	−1.8	−5.3
Hybrid **2**	−1.4	−2.9	−8.7
Hybrid **3**	−1.6	−8.1	−24.4
Hybrid **4**	−1.5	−11.7	−35.2
Hybrid **5**	−2.4	−7.5	−22.5

(Table 3) obtained from eq 5, suggesting that our model regarding the packing of hybrids into vesicles is reasonable. Then, the chemical potential difference between a hybrid surfactant in vesicle and in solution ($\Delta^0\mu$) is calculated as $-23.4 \ k_B T$ from:[32]

$$X_{cac} \approx e^{\Delta\mu°/k_b T} \qquad (8)$$

The hybrid that shows a greater slope in Figure 7 indicates a larger u value (i.e., a stronger attraction among unimers). The volume, length, and rigidity of the organic linker might control the curvature of the vesicles and prescribe the structure according to the behavior of conventional surfactants.[31] For the first three hybrids with similar organic linkers, hybrid **3** possesses the highest hydrophobicity and weakest rigidity. Consequently, it has the most negative u value, consistent with its lowest cac value. Hybrid **4** has bulky aromatic rings and the largest distance between two polar headgroups (ca. 1.60 nm). We consider that this space is enough to allow these $\pi-\pi$ associations. In comparison, hybrid **5** presents the most hydrophobic organic linker among these hybrids. However, the distance between two polar headgroups probably is not enough to allow intermolecular associations through the middle part as a result of the electronic repulsions between the adjacent POM groups on the vesicle surface. In such a case, we speculate that the TBA countercations get involved in vesicle formation by contributing their alkyl chains to the hydrophobic layers of the vesicles. This is confirmed by the low apparent charge density (from the ζ potential); its u value is in a reasonable range. That is, the counterions for hybrid **5** seem to interact with the hybrid clusters more closely than with the others in a given solvent. As a result, hybrid **5** starts to form vesicles in solvents with relatively low acetone contents. A possible reason is that in **5** the hydrophobic domain is so dominant that it attracts more TBA counterions to the hydrophobic region.

Bending and Edge Interchange Energies and the Role of the Elastic Constant. Vesicle formation involves the competition between the bending energy and the elastic modulus.[33,34] The so-called elastic constants, including the spontaneous curvature (LC_{sp}), the elastic modulus (k_c), and the Gaussian bending constant (k'_c), can be applied to describe the properties of surfactant films and to predict the vesicle size.[35] For example, the k_c values for phospholipid systems lie in the range of 1−20- ($k_B T$);[36,37] for SDS, it is $7.06 k_B T$ ($T = 298$ K).[38] These values can serve as a reference to clarify the similarities and differences between the conventional surfactants and the hybrids.

Our current systems are much more complicated, with special polar headgroups, mixed solvents, various organic linkers, and large amphiphilic counterions. For example, adding one more $-CH_2-$ group to the middle linker increases the linker's
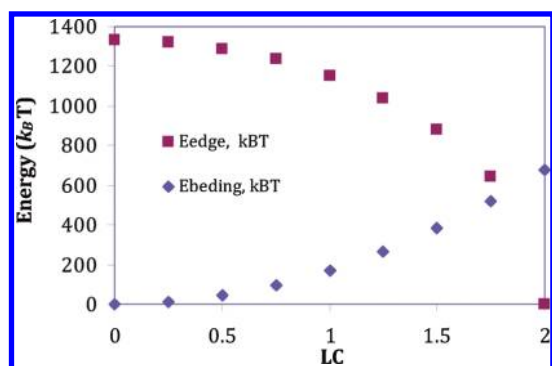
Figure 8. Competition between the edge energy and the bending energy for hybrid **5** during vesicle formation.

flexibility and hydrophobicity, and adding aromatic rings increases the linker's rigidity. On the basis of a theoretical model proposed by Liposwsky,[39] the bending and edge energies for the vesicle formation of these hybrids are calculated for spherical cap geometry respectively by

$$E_{bend} = 2\pi k_c (LC - LC_{sp})^2 \qquad (9)$$

$$E_{edge} = 2\pi L \lambda \sqrt{1 - (LC/2)^2} \qquad (10)$$

with C being the vesicle curvature $(1/R_{h,0})$, L $(= 2R_{h,0})$ being the length of the film, and λ being the edge energy per unit length (with a value of 1×10^{-20} J/nm).[36]

One important property of these dumbbell hybrids is their symmetrical anionic polar heads, with which we can treat the spontaneous curvature (C_{sp}) as zero. Also, complete vesicle formation is achieved at LC = 2. Consequently, eq 9 is simplified to[40]

$$E_{bend} = \frac{8\pi k_c}{2} = 4\pi k_c \qquad (11)$$

In eq 11, the 2 in the denominator implies that the vesicles formed by hybrids have only one layer of monomers instead of two layers for conventional surfactants.

A common vesicle-formation process starts from membrane formation. As the membrane grows in size, the edge energy increases because of the increased exposure of the solvophobic edge to the solvent until it reaches a critical value, followed by a bending process when the edge energy exceeds the bending energy. When the curvature of the membrane reaches a critical value $(LC_{critical})$ of ~1.8, the membrane will close spontaneously to form a complete spherical vesicle.[41] Figure 8 shows the competition between bending energy and edge energy for hybrid **5** to form vesicles.

$\pi-A$ isotherms (described in detail in Figure 11) and eq 12 are used to calculate the elastic constants and bending energies. The 2D surface compression modulus (Cs^{-1}) is referred as the equilibrium in-plane elastic modulus.[42] Also, Cs^{-1} was defined by Davis[43] to make possible comparisons with elastic modulus of area compressibility values[44]

$$Cs^{-1} = A(\partial\pi/\partial A)_T \qquad (12)$$

where A is the area of the monolayer at $\pi = 0$ and $(\partial\pi/\partial A)_T$ is the slope in the liquid condensed phase.

For comparison, the SDS anionic surfactant has a bending-energy value of ca. $90k_BT$ and forms small-radius micelles of ca. 1.8 nm.[45] However, vesicles from cationic—anionic (catanionic) surfactants such as SOS/CTAB presents a bending energy of $610k_BT$; correspondingly, vesicles with $R_h \approx 20$ nm are formed.[46] The vesicles formed by these hybrids have bending-energy values similar to those of catanionic vesicles, but they are significantly larger. We speculate that this difference is due to the special molecular morphologies of the hybrids and the amphiphilic countercations. The dumbbell shape enables the hybrids to form bilayer structures by using one layer of molecules, which increases the rigidity of the membrane and consequently the bending energy, leading to the formation of larger vesicles. In addition, the TBA counterions might participate in vesicle formation by contributing their alkyl chains to the hydrophobic domains, which again increases the membrane rigidity.

With a dominant bending energy, the precursor membranes could be larger. Consequently, the elastic modulus would also increase, resulting in larger vesicles. As shown in Figure 9A, the hybrid vesicle size increases with increasing elastic modulus. In addition, Figure 9B shows the effect of hybrid lengths on the elastic modulus, where a linear relationship is observed for the hybrids containing alkyl-amide groups. Hybrid **4**, with aromatic rings, does not follow the trend because of its rigid aromatic groups.

Effect of Electrostatic Interactions on the Vesicle's Elastic Properties. The charge effect on the bending constants of surface membranes indicates that the elastic constant varies with the surface charge density or surfactant concentration.[47] The elastic modulus due to the electric interaction k_c^{ele} increases until the surface charge is completely saturated. However, Gauss modulus k'_c^{ele} decreases (becomes more negative) with increasing surface charge. In our current case, each hybrid contains 10 negative charges. Winterhalter and Helfrich[48] proposed to calculate the electric contribution to the bending modulus by

$$k_c^{ele} = \frac{\sigma^2(1+\delta^2)}{\varepsilon_w\chi}\frac{3}{4\chi^2} \qquad (13)$$

$$k'_c^{ele} = -\frac{\sigma^2(1+\delta^2)}{\varepsilon_w}\left(\frac{1}{2\chi^2} + \frac{d}{2\chi}\right) \qquad (14)$$

where the superscript "ele" refers to the electrostatic contributions without taking into considerations other forces such as van der Waals forces. The surface charge density σ is given in C/m²; 2δ is the surface charge difference between the inner and outer monolayers (negligible here), d is the monolayer membrane thickness (head-to-head distance for the hybrids here), ε_w is the dielectric constant of water, and χ is the Debye screening length.

The surface charge was calculated using the Hückel equation

$$\mu_0 = \frac{q}{6\pi\eta r} \qquad (15)$$

where μ_0, q, η, and r are the absolute mobility of particles, the effective charge on particles, the solvent viscosity, and the particle radius, respectively.[49]

The five hybrids have the same polar headgroups and charges; therefore, similar contributions from electrostatic interaction to the bending modulus (k_c^{ele}) of their vesicles can be expected. However, their k_c^{ele} and effective surface charges are clearly different (Figure 10). A linear relationship between the effective surface charge density and k_c^{ele} is observed, suggesting that the
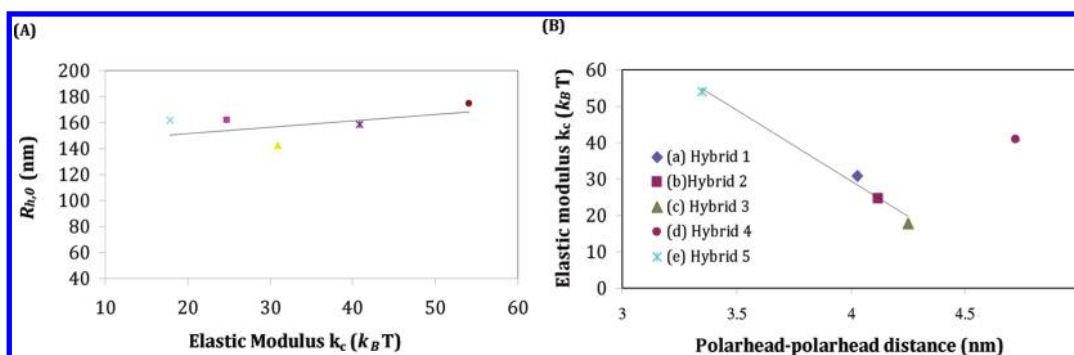
Figure 9. (A) Vesicle size increases with increasing elastic modulus of the hybrids. (B) Relation between the hybrid length and the elastic modulus.
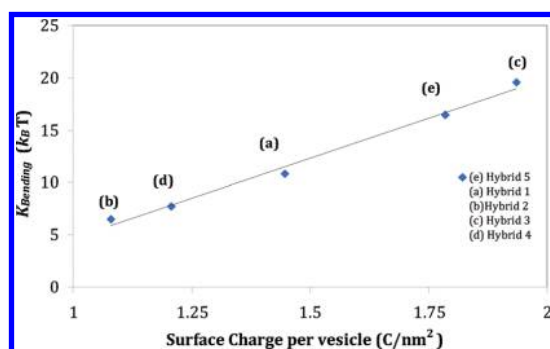

Figure 10. Influence of the surface charge per vesicle (σ) and its effect in forming vesicular structures at 25 °C. (a) Hybrid **1**, (b) hybrid **2**, (c) hybrid **3**, (d) hybrid **4**, and (e) hybrid **5**.

TBA counterions have different degrees of association to different hybrids, and the degree of association makes a significant contribution to the bending energy of vesicle formation.

The electrostatic and elastic properties of the vesicles formed by five hybrids are summarized in Table 4. The invagination length ($\xi = k_c/\lambda$) sets the length scale at which we expect to find the first membrane development stage showing the potential to form vesicles.[50] The invagination lengths for hybrids **1**−**3** have similar values (12 ± 3 nm), close to the estimated value for phospholipid membranes (6.9−10 nm).[51] In contrast, the invagination lengths for hybrids **4** and **5** are almost doubled, possibly attributed to their more rigid organic linkers, which results in more rigid membranes.

Finally, the stability of the vesicles is dictated by the value of $2k_c^{ele} + k_c'^{ele}$. The vesicles are stable if the value is positive and unstable if the value is negative.[52] Here, all of the $2k_c^{ele} + k_c'^{ele}$ values are >0, suggesting that the hybrid vesicles are stable in solution.

Dumbbell-Shaped Hybrid Surfactants at the Water/Vapor Interface. Water/air (L/A) interfacial behavior is important in understanding the nature of surfactants such as solvophobicity and miscibility in the liquid subphase (water). Early studies on traditional amphiphiles showed the importance of the length of hydrophobic chains on the L/A behavior.[53] Poly(ethylene oxide) (PEO) nonionic surfactants show a vertical orientation of the ethylene oxide (EO) chains, and the surface films become more expanded with increasing EO length.[54] However, for anionic surfactant sodium alkylbenzene sulfonates, the area per molecule at the interface decreases with increasing molecular weight. The van der Waals forces between the alkylbenzene tails increase with increasing chain length, indicating that the surfactant with longer alkylbenzene chains can be more easily compressed.[54]

The hybrids at the water/air interface are studied with the Langmuir−Blodgett technique.[55] Figure 11 shows the five corresponding π−A isotherms. The calculated molecular area at the interface and the shape and phase transitions for each hybrid are quite different; even the five hybrids share the same type of polar headgroups, indicating the effect of the organic linkers. Isotherms for hybrids **1** and **2** (Figure 11A) exhibit the typical behavior of a liquid expanded (LE) phase without reaching the condensed phase transition plateau, suggesting that these hybrids cannot form a compact monolayer at the interface (Figure 12A). In contrast, hybrid **3** presents two well-defined phases, an LE phase and a liquid condensed (LC) phase coupled with a pronounced plateau allowing the coexistence of both phases and a collapse pressure at 100 Å^2. The LC phase indicates the formation of an interfacial compact monolayer. It is reasonably speculated that the hybrids should use one of their headgroups to stay in the water phase whereas the whole molecule will stand up at the interface upon closely interacting with their neighboring hybrids. The other headgroup should stay in the air (Figure 12B,C). The geometrical constraints of the molecules do not allow both headgroups to stay in the aqueous solution during close packing. Overall, these three hybrids exhibit interfacial behavior similar to that of some cationic gemini surfactants containing two amphiphilic moieties connected by spacer groups. In both cases, the isotherm curve moves to the right side with increasing length of the spacer group, indicating a larger interfacial area for each amphiphile (i.e., they spread out further at the interface).[56] Besides hydrophobic interactions, electrostatic interactions and hydrogen bonding might also affect the surface pressure.[57] Here, the hybrids have very limited solubility in water, suggesting very weak hydrogen bonding formation between the linkers, and the contribution from the electrostatic interaction should be the same for all of the hybrids. Therefore, the differences in the isotherm curves among the hybrids should be due to the hydrophobic interaction between their organic linkers.

Both π−A isotherms for hybrids **4** and **5** present LE and LC phases connected to a plateau (Figure 11B). The LE interfacial areas per molecule, obtained by extrapolation to zero pressure for hybrids **4** and **5**, are 205 and 348 Å^2, respectively. This difference could be due to the fact that hybrid **4** possesses rigid π−π bonds that may create significant attractive interactions. In some cationic gemini surfactant systems, the π−π interactions from aromatic functional groups can promote the formation of networks or self-associations.[58,59] In addition, the rigid molecular architectures of these hybrids limit their expansion at the interface; therefore, more compressed isotherms are obtained.

Table 4. Electrostatic and Elastic Properties of the Five Hybrid Surfactants[a]

	hybrid **1**	hybrid **2**	hybrid **3**	hybrid **4**	hybrid **5**
conc (mg/mL)	1.0	1.0	1.0	1.0	1.0
ξ (nm)	12.7	10.2	13.2	16.8	22.3
σ (A·s/m^{2}x10^{-4})	1.79	1.45	1.04	0.92	1.21
k_c (k_BT)	30.9	24.7	17.8	40.8	54.1
k_c^{ele} (k_BT)	10.9	6.1	4.4	7.7	16.4
$k'_c{}^{ele}$ (k_BT)	−7.5	−4.2	−3.0	−5.4	−11.3
λ (J/nm × 10^{-20})	1.00	1.00	1.00	1.00	1.00
$E_{bend} = 4\pi k_c$ (k_BT)	389	310	224	512	680
E_{edge} (k_BT)	1089	1233	1183	1206	1331
$E_{ves}^{ele} = 2\pi(2k_c^{ele} + k'_c{}^{ele})$ (k_BT)	89.3	49.9	36.2	63.3	136

[a] The test conditions were water/acetone at 50 vol % content and 25 °C.
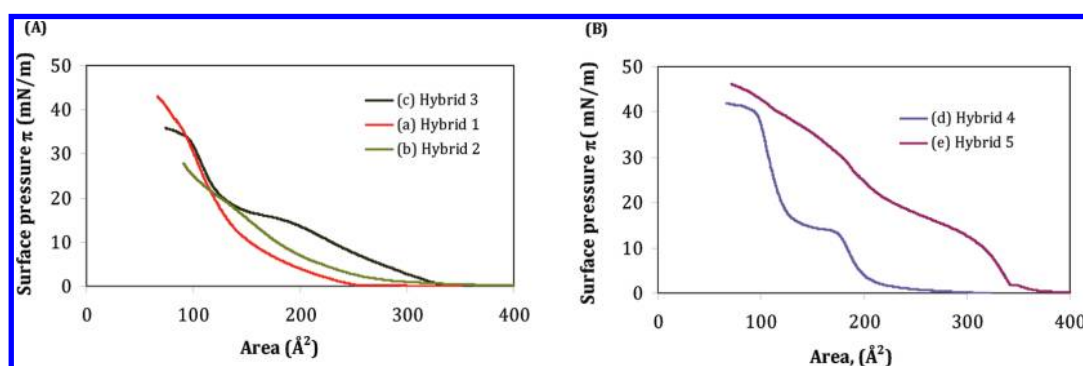

Figure 11. Surface pressure π–A isotherms on a water subphase. The *LC* area/molecule values are 160, 230, 174, 146, and 300 Å^2 for hybrids **1**–**5**, respectively. All of the isotherms collapse around 100 Å^2, which is the cross-sectional area for all of these hybrid surfactants.
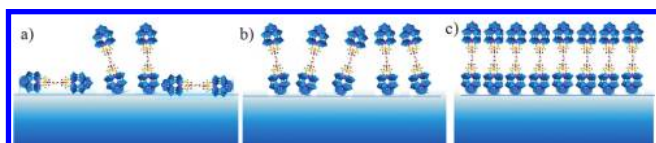

Figure 12. Monolayer formation for the dumbbell-shaped hybrid surfactants at the water/vapor interface: (a) LE/G phase, (b) LE phase, and (c) LC phase. TBA counterions are not shown but might play a role by being located between the polar headgroups to screen and decrease the electrostatic repulsion.

Overall, the hybrids indeed demonstrate interfacial behavior similar to that of some ionic surfactants. However, their less-hydrophilic headgroups, unique molecular architecture, and rigid molecular structures make it more difficult for them than for conventional surfactants to form ordered interfacial monolayers.

The TBA counterions are expected to affect the interfacial behavior described above. We speculate that the TBA cations might also stay at the interface (reasonable if considering that they are also amphiphilic) and between POM groups to help to decrease the electrostatic repulsion among them.

■ CONCLUSIONS

The self-assembly of five polyoxometalate-based dumbbell-shaped inorganic—organic—inorganic hybrids into bilayer vesicles is observed in selected polar solvents. These hybrids all have two identical Wells—Dawson-type POM clusters connected by different organic linkers. Vesicle formation is entropy-driven and charge-regulated. The hydrophobicity, overall length, and shape of the middle organic linkers in the hybrids play important roles in determining the properties of the vesicles (e.g., the size, cac, thermodynamic parameters, cohesive bond energies, bending/edge energies, and elastic modulus).

The organic linkers also control the behavior of hybrids at the water/air interface. From the π–A isotherms, the packing of hybrids into a monolayer at the interface becomes more ordered when the linker becomes more hydrophobic. Liquid expanded and liquid condensed phases are clearly located and connected through a plateau, suggesting that the hybrids behave similarly to some cationic gemini surfactants that possess similar molecular architectures. Overall, the hybrids demonstrate a weaker capability of forming monolayers at the interface.

In summary, the POM—organic hybrids indeed demonstrate certain typical amphiphilic behaviors in polar solvents. Their large, rigid polar headgroups and unique molecular architecture render their self-assembly with new features such as the very high entropy gain. The involvement of the amphiphilic counterions in the self-assembly and the different organic linkers make the self-assembly behavior highly adjustable. With similar molecular architectures, these hybrid surfactants demonstrate similar and predictable self-assembly behaviors, which will certainly enrich the family of amphiphilic surfactants and at the same time expand the applications of the POM materials to organic media.

■ AUTHOR INFORMATION

Corresponding Authors
*E-mail: lee.cronin@glasgow.ac.uk, liu@lehigh.edu.

■ REFERENCES

(1) Hill, C. L. *Chem. Rev.* **1998**, *98*, 1.

(2) (a) Proust, A.; Thouvenot, R.; Gouzerh, P. *Chem. Commun.* **2008**, 1837. (b) Dolbecq, A.; Dumas, E.; Mayer, C. R.; Mialane, P. *Chem. Rev.* **2010**, *110*, 6009.

(3) (a) Hou, Y. Q.; Hill, C. L. *J. Am. Chem. Soc.* **1993**, *115*, 11823. (b) Zeng, H.; Newkome, G. R.; Hill, C. L. *Angew. Chem., Int. Ed.* **2000**, *39*, 1771.

(4) Song, Y.-F.; McMillan, N.; Long, D. L.; Thiel, J.; Ding, Y.; Chen, H.; Gadegaard, N.; Cronin, L. *Chem.—Eur. J.* **2008**, 14.

(5) Sanchez, C.; Soler-Illia, G. J. D. A. A.; Ribot, F.; Grosso, D. *Comptes. Rendus. Chimie* **2003**, *6*, 1131.

(6) Yuan, L.; Qin, C.; Wang, X.; Wang, E.; Chang, S. *Eur. J. Inorg. Chem.* **2008**, *31*, 4936.

(7) Finn, R.; Zubieta, J. *J. Inorg. Chem.* **2001**, *40*, 2466.

(8) Micoine, K.; Hasenknopf, B.; Thorimbert, S.; Lacôte, E.; Malacria, M. *Angew. Chem., Int. Ed.* **2009**, *48*, 3466.

(9) Zhu, Y.; Xiao, Z.; Ge, N.; Wang, N.; Wei, Y.; Wang, Y. *Cryst. Growth Des.* **2006**, *6*, 1620.

(10) Lee, C. F.; Leigh, D. A.; Pritchard, R. G.; Schultz, D.; Teat, S. J.; Timco, G. A.; Winpenny, R. E. P. *Nature* **2009**, *458*, 314.

(11) Song, Y. F.; Abbas, H.; Ritchie, C.; McMillian, N.; Long, D.-L.; Gadegaard, N.; Cronin, L. *J. Mater. Chem.* **2007**, *17*, 1903.

(12) Lu, M.; Wei, Y.; Xu, B.; Cheung, C.; Peng, Z.; Powell, D. *Angew. Chem., Int. Ed.* **2002**, *41*, 1566.

(13) Zhang, J.; Song, Y.-F.; Cronin, L.; Liu, T. *J. Am. Chem. Soc.* **2008**, *130*, 14408.

(14) Zhang, J.; Song, Y.-F.; Cronin, L.; Liu, T. *Chem.—Eur. J.* **2010**, *16*, 11320.

(15) (a) Landsmann, S.; Lizandara-Pueyo, C.; Polarz, S. *J. Am. Chem. Soc.* **2010**, *132*, 5315. (b) Han, Y.; Xiao, Y.; Zhang, Z.; Liu, B.; Zheng, P.; He, S.; Wang, W. *Macromolecules* **2009**, *42*, 6543.

(16) Pradeep, C. P.; Misdrahi, M.; Li, F.; Zhang, J.; Xu, L.; Long, D. L.; Liu, T.; Cronin, L. *Angew. Chem., Int. Ed.* **2009**, *48*, 8309.

(17) Pradeep, C. P.; Li, F.; Lydon, C.; Miras, H.; Long, D. L.; Xu, L.; Cronin, L. *Chem.—Eur. J.* **2011**, *17*, 7472.

(18) Hiemenz, P.; Rajagopalan, R. *Principles of Colloid and Surface Chemistry*; Marcel Dekker: New York, 1997.

(19) Provencher, S. *Biophys. J.* **1976**, *16*, 29.

(20) Liu, T.; Diemann, E.; Li, H.; Dress, A.; Müller, A. *Nature* **2003**, *426*, 59.

(21) Barton, A. F. M. *Handbook of Solubility Parameters and Other Cohesion Parameters*; CRC Press: Boca Raton, FL, 1983.

(22) Hansen, C. M. *Hansen Solubility Parameters: A User's Handbook*; CRC Press: Boca Raton, FL, 2007.

(23) Small, P. *J. Appl. Chem.* **1953**, *3*, 71.

(24) Liu, T.; Zhou, Z.; Wu, C.; Nace, V.; Chu, B. *J. Phys. Chem. B* **1998**, *102*, 2875.

(25) Meguro, K.; Takasawa, Y.; Kawahashi, Y.; Tabata, Y.; Ueno, M. *J. Colloid Interface Sci.* **1981**, *82*, 50.

(26) Volkov, V. *Colloid J. USSR* **1976**, *38*, 610.

(27) Ao, M.; Huang, P.; Xu, G.; Yang, X.; Wang, Y. *Colloid Polym. Sci.* **2009**, *287*, 395.

(28) Liu, G.; Liu, T. *Langmuir* **2005**, *21*, 2713.

(29) Verhoeff, A.; Kistler, M.; Bhatt, A.; Pigga, J.; Groenewold, J.; Klokkenburg, M.; Veen, S.; Roy, S.; Liu, T.; Kegel, W. K. *Phys. Rev. Lett.* **2007**, *99*, 066104.

(30) Qi, W.; Wang, M.; Xu, G. *Chem. Phys. Lett.* **2003**, 632.

(31) Evans, D. F.; Ninham, B. W. *J. Phys. Chem. B* **1986**, *90*, 226.

(32) Israelachvili, J. *Intermolecular and Surface Forces*, 2nd ed.; Academic Press: San Diego, 1992.

(33) Claessens, M.; Leermakers, F.; Hoeskstra, F.; Cohen, S. *J. Phys. Chem. B* **2007**, *111*, 7127.

(34) Xia, Y.; Goldmints, I.; Johnson, P.; Hatton, A.; Bose, A. *Langmuir* **2002**, *18*, 3822.

(35) Bergström, L. M. *Langmuir* **2006**, *22*, 3678.

(36) Evans, E.; Rawicz, W. *Phys. Rev. Lett.* **1990**, *64*, 2094.

(37) Fennell, D.; Wennerström., H. *The Colloidal Domain Where Physics, Chemistry, and Biology Meet*, 2nd ed.; Wiley-VCH: New York, 1999.

(38) Bergström, L.; Eriksson, J. *Langmuir* **1996**, *12*, 624.

(39) Lipowsky, R. *J. Phys. II France* **1992**, *2*, 1825.

(40) Antonietti, M.; Forster, S. *Adv. Mater.* **2003**, *15*, 1323.

(41) Inoue, T. *Interaction of Surfactants with Phospholipid Vesicles*; Marcel Dekker: New York, 1996; Vol. 62.

(42) Pavinatto, F.; Caseli, L.; Pavinatto, A.; Dos Santos, D.; Nobre, T.; Zaniquelli, M.; Silva, H.; Miranda, P.; Oliveira, O. R. *Langmuir* **2007**, *23*, 7666.

(43) Davies, J. T.; Rideal, E. K. *Interfacial Phenomena*; Academic Press: New York, 1993.

(44) Krael, J.; Li, J.; Miller, R.; Bree, M.; Kretzschmar, G.; Mohwald, H. *Colloid Polym. Sci.* **1996**, *274*, 1183.

(45) Suarez, A.; Sandez, M.; Gil, A. *Colloid Polym. Sci.* **1995**, *273*, 876.

(46) Shioi, A.; Hatton, A. *Langmuir* **2002**, *18*, 7341.

(47) May, S. *J. Chem. Phys.* **1996**, *105*, 8314.

(48) Winterhalter, M.; Helfrich, W. *J. Phys. Chem. B* **1988**, *92*, 6865.

(49) Kistler, M.; Bhatt, A.; Liu, G.; Casa, D.; Liu, T. *J. Am. Chem. Soc.* **2007**, *129*, 6453.

(50) Semrau, S.; Idema, T.; Schmidt, T.; Storm, C. *Biophys. J.* **2009**, *96*, 4906.

(51) Schick, M. *J. Colloid Sci.* **1962**, *17*, 801.

(52) Daicic, J.; Fogden, A.; Carlsson, I.; Wennerstrom, H.; Jonsson *Phys. Rev. E: Stat., Nonlinear, Soft Matter Phys.* **1996**, *54*, 3984.

(53) Wang, Y.; Pereira, C.; Marques, E.; Brito, R.; Ferreira, E.; Silva, F. *Thin Solid Films* **2006**, *515*, 2031.

(54) Meader, A.; Criddle, D. *J. Colloid Sci.* **1953**, *8*, 170.

(55) Talham, D.; Yamamoto, T.; Meisel, M. *J. Phys.: Condens. Matter* **2008**, *20*, 184006.

(56) Chen, Q.; Zhang, D.; Li, R.; Liu, H.; Hu, Y. *Thin Solid Films* **2008**, *516*, 8782.

(57) Gole, A.; Dash, C.; Mandale, A.; Rao, M.; Sastry, M. *Anal. Chem.* **2000**, *72*, 4301.

(58) Cheng, Q.; Liang, X.; Wang, S.; Xu, S.; Liu, H.; Hu, Y. *J. Colloid Interface Sci.* **2007**, *314*, 651.

(59) Gron, F.; Klein, K.; Koynov, K. *Macromol. Rapid Commun.* **2010**, *31*, 78.